THE JOURNAL OF BIOLOGICAL CHEMISTRY VOL. 289, NO. 24, pp. 16736–16747, June 13, 2014

Glucose Starvation Inhibits Autophagy via Vacuolar Hydrolysis and Induces Plasma Membrane Internalization by Down-regulating Recycling*[S]

Received for publication, October 15, 2013, and in revised form, April 16, 2014 Published, JBC Papers in Press, April 21, 2014, DOI 10.1074/jbc.M113.525782

Michael J. Lang[‡], Jorge Y. Martinez-Marquez[‡], Derek C. Prosser[§], Laura R. Ganser[¶], Destiney Buelto[‖1], Beverly Wendland[§], and Mara C. Duncan[‡¶‖2]

From the [‡]Department of Cell and Developmental Biology, the University of Michigan, Ann Arbor, Michigan 48109, the [¶]Department of Biology, the University of North Carolina, Chapel Hill, North Carolina 27599, the [§]Department of Biology, the Johns Hopkins University, Baltimore, Maryland 21218, and the [‖]Curriculum in Genetics and Molecular Biology, the University of North Carolina, Chapel Hill, North Carolina 27599

Background: During energy starvation, cells utilize intracellular resources for survival; however, the resources used during glucose starvation are unknown.
Results: In glucose-starved yeast, vacuolar hydrolysis and endocytosis promote survival whereas autophagy is dispensable.
Conclusion: Vacuolar hydrolysis blocks autophagy and provides resources for survival during glucose starvation.
Significance: This new survival mechanism could protect cells from starvation in many situations.

Cellular energy influences all aspects of cellular function. Although cells can adapt to a gradual reduction in energy, acute energy depletion poses a unique challenge. Because acute depletion hampers the transport of new energy sources into the cell, the cell must use endogenous substrates to replenish energy after acute depletion. In the yeast *Saccharomyces cerevisiae*, glucose starvation causes an acute depletion of intracellular energy that recovers during continued glucose starvation. However, how the cell replenishes energy during the early phase of glucose starvation is unknown. In this study, we investigated the role of pathways that deliver proteins and lipids to the vacuole during glucose starvation. We report that in response to glucose starvation, plasma membrane proteins are directed to the vacuole through reduced recycling at the endosomes. Furthermore, we found that vacuolar hydrolysis inhibits macroautophagy in a target of rapamycin complex 1-dependent manner. Accordingly, we found that endocytosis and hydrolysis are required for survival in glucose starvation, whereas macroautophagy is dispensable. Together, these results suggest that hydrolysis of components delivered to the vacuole independent of autophagy is the cell survival mechanism used by *S. cerevisiae* in response to glucose starvation.

Glucose is the preferred energy source for many proliferating cells, including the yeast *Saccharomyces cerevisiae.* To utilize glucose, yeast adopts a specific metabolic program, which is similar to the Warburg metabolism seen in cancer and stem cells (1). In this program, the cell shuts down systems that allow utilization of energy sources other than glucose. It forgoes storage of carbohydrates or amino acids and instead utilizes these nutrients directly for growth. Furthermore, this program inhibits ATP generation by the mitochondria; ATP is derived primarily from glycolysis. Consequently, a precipitous drop in ATP levels follows glucose starvation (2, 3). With no reserves and little ATP to facilitate import of new catabolic substrates from extracellular sources, the cell likely hydrolyzes endogenous cellular components to overcome the ATP deficit during the initial phases of glucose starvation.

Macroautophagy (hereafter autophagy) is an important catabolic process activated by various types of starvation. In autophagy, cellular cytoplasm and organelles are engulfed in a double-membraned structure called the autophagosome (for review, see Ref. 4). Fusion of the autophagosome with the lysosome (vacuole in yeast) leads to hydrolysis of the enclosed cellular components. This mechanism allows the cell to recycle amino acids, lipids, and nucleotides for use as energy sources and for new biosynthesis. Three conserved metabolic kinases regulate autophagy. The AMP-activated kinases (AMPKs)[3] activate autophagy whereas protein kinase A (PKA) and the target of rapamycin complex 1 (TORC1) inhibit autophagy (for review, see Ref. 5). During glucose starvation, AMPK is activated whereas PKA is inhibited (3, 6). These effects suggest that autophagy may occur during glucose starvation. However, autophagy genes are dispensable for glucose survival (7). This indicates that the cell must use additional mechanisms to replenish nutrient stores during glucose starvation. The process that cells use to survive in the absence of autophagy is unknown.

One possible alternative to autophagy is the degradation of proteins that are delivered to the vacuole from the endosomes. This pathway promotes cell survival during amino acid starvation (8). Furthermore, in response to acute glucose starvation, proteins involved in endosomal sorting become cytosolic.

* This work was supported, in whole or in part, by National Institutes of Health Grant GM092741 (to M. C. D.) and GM60979 (to B. W.) through the NIGMS.
[S] This article contains a supplemental Data Base.
[1] Supported by National Institutes of Health Grant T32 709237.
[2] To whom correspondence should be addressed: Dept. of Cell and Developmental Biology, The University of Michigan, 109 Zina Pitcher Pl., Ann Arbor, MI 41809. Tel.: 734-763-4106; E-mail: mcduncan@umich.edu.

[3] The abbreviations used are: AMPK, AMP-activated kinase; CME, clathrin-mediated endocytosis; TORC1, target of rapamycin complex 1.

TABLE 1
Strains used

Strain	Genotype	Source
BY4741	MAT a *his3Δ1 leu2Δ0 ura3Δ0 met15Δ0*	Invitrogen
BY4742	MAT α *his3Δ1 leu2Δ0 ura3Δ0 lys2Δ0*	Invitrogen
DLY046	BY4742 *SUR7-GFP::KanMx*	This study
DLY050	BY4742 *HXT3-GFP::KanMx*	This study
DLY052	BY4742 *VHT1-GFP::KanMx*	This study
DLY055	BY4742 *RAX2-GFP::KanMx*	This study
MDY1113	BY4741 *FET3-GFP::HIS3Mx*	This study
QAY559	BY4742 *PMA1-mCherry::HIS3Mx*	This study
QAY561	Diploid *his3Δ1/his3Δ1 leu2Δ0/leu2Δ0 MET15+/met15Δ0 Lys2+/lys2Δ0 ura3Δ0/ura3Δ0 GAP1-GFP::HIS3Mx*	This study
MDY543	BY4741 *TAT1-GFP::His3Mx*	Invitrogen
MDY902	BY4741 *STE2-GFP::HIS3Mx*	Invitrogen
DLY594	BY4742 *sla1Δ::HIS3Mx TAT1-GFP::KanMx*	This study
MDY1119	BY4742 *vps4Δ::KanMx*	Invitrogen
DLY269	BY4742 *pep4Δ::KanMx*	Invitrogen
MDY1117	BY4742 *atg5Δ::KanMx*	Invitrogen
DLY085	BY4742 *vph1Δ::KanMx*	Invitrogen
DLY118	BY4742 *sla1Δ::HIS3Mx*	This study
DLY120	BY4742 *rvs161Δ::HIS3Mx*	This study
DLY234	BY4742 pRS315-*GFP-SNC1*	This study
BWY2497	MATα *his3-Δ200 trp1-Δ901 leu2–3,112 ura3–52 lys2–801 suc2-Δ9 ent1Δ::LEU2 ent2Δ::HIS3 yap1801Δ::HIS3 yap1802Δ::LEU2 + pBW0768 (pEnt1 [CEN TRP1])*	Ref. 14
BWY3817	MATα *his3-Δ200 trp1-Δ901 leu2–3,112 ura3–52 lys2–801 suc2-Δ9 MUP1-GFP::KanMx*	Ref. 15
BWY4892	BWY3817 *MUP1-GFP::KanMx ent1Δ::LEU2 ent2Δ::HIS3 yap1801Δ::HIS3 yap1802Δ::LEU2* + pBW0768 (pEnt1 [CEN *TRP1*])	This study; derived from BWY2497 and BWY3817
BWY4893	BWY3817 *MUP1-GFP::KanMx ent1Δ::LEU2 ent2Δ::HIS3 yap1801Δ::HIS3 yap1802Δ::LEU2* + pBW0778 (pENTH1 [CEN *TRP1*])	This study; derived from BWY2497 and BWY3817
TN215	MATa *ade2 his3 leu2 lys2 trp1 ura3 pho8::pho8Δ60*	Ref. 13
LWY114	MAT α *ura3–52*	Lois Weisman laboratory strain
FY4	Mat a prototroph	Ref. 16
DLY432	Mat a *pep4Δ::kanMx ura3Δ0*	This study; derived from FY4 and DLY269
DLY434	Mat a ura3Δ0	This study; derived from FY4 and DLY269
NSY125	Mat a *his4–539am lys2–801am ura3–52*	Ref. 28
NSY657	Mat a *his4–539am lys2–801am ura3–52 rcy1::KanMx*	Ref. 28

However, proteins involved in endocytosis remain membrane-associated (9, 10). This could cause proteins endocytosed from the plasma membrane to be directed to intracellular compartments rather than getting recycled back to the membrane. Indeed, glucose starvation directs internalization of plasma membrane proteins that seem unrelated to glucose metabolism, such as the uracil permease, Fur4, and the hydrophobic amino acid permease, Tat2 (11, 12). This suggests that glucose starvation may alter traffic within the endosomal system. In this study, we investigated the roles of endocytosis, endosomal membrane traffic, and autophagy in ensuring survival during glucose starvation.

EXPERIMENTAL PROCEDURES

Chemicals—Phenylmethanesulfonylfluoride (PMSF) and rapamycin were from Sigma. FM4-64 was from GE Healthcare.

Strains and Plasmids—Strains are listed in Table 1 (13–16). Deletion strains from systematic collections were verified by PCR utilizing primers outside of the deletion cassette. GFP strains from systematic collections were verified by microscopy. Strains in this study were generated using a PCR-based strategy with pFA6a-S65TGFP-KanMX, pFA6a-S65T-GFP-His3Mx, pFA6a-mCherry-His3Mx, pFA6a-KanMx, pRS303, or pRS305 as described previously (17). Plasmids pRS316 GFP-Aut7 (Atg8), pADHU-GFP-cSNC1, pBW0768 (pEnt1 [CEN TRP1], and pBW0778 (pENTH1 [CEN TRP1]) were described previously (18–20).

Growth Conditions—Media compositions used are listed in Table 2. Except where noted, add-back mix contains 0.54 mM adenine (adenine sulfate), 0.76 mM L-leucine, 0.55 mM L-lysine, 0.49 mM L-tryptophan, 0.32 mM L-histidine, 0.45 mM uracil, and 0.13 mM L-methionine. Nucleotide only add-back mix contains only 0.54 mM adenine (adenine sulfate) and 0.45 mM uracil. For cells expressing *GFP-ATG8,* uracil was omitted from add-back mix. For cells expressing *MUP1-GFP*, methionine was omitted from add-back mix to induce expression.

With the exception of media for FET3-GFP, yeast nitrogen base was the Wickerham formula, without amino acids and ammonium sulfate, used at the manufacturer recommended concentrations (BD Biosciences). For FET3-GFP, yeast nitrogen base lacking iron was used (Formedium, Hunstanton, UK). Unless otherwise indicated, cells were grown in replete medium for 72 h, maintaining the culture at a low density. For starvation, cells at mid-logarithmic (log) phase (A_{600}~0.2–0.5) were pelleted and washed three times with the appropriate starvation media indicated in Table 2 then incubated at 30 °C for the indicated times.

FM4-64 Assays—To assess initial rates of endocytosis, cells grown to log phase or starved at different time points were pelleted and resuspended in appropriate media supplemented with 0.4 μg/ml FM4-64. After 2.5 min, a stop mix was added to a final concentration of 10 mM sodium fluoride and sodium azide, and cells were placed on ice. Unbound FM4-64 was removed with three washes in ice-cold media containing 10 mM sodium fluoride and sodium azide. Cells were kept on ice until imaged. To assess FM4-64 accumulation and delivery to the vacuole, cells grown to log phase or starved at different time points were pelleted and resuspended in appropriate media supplemented with 0.4 μg/ml FM4-64 at room temperature.

TABLE 2
Formulations of media used

Component	Replete	Glucose starvation	Glucose and Nitrogen starvation	Nitrogen starvation
Yeast nitrogen base	Added	Added	Added	Added
Nitrogen source	38 mM ammonium sulfate[a]	38 mM ammonium sulfate[a]	None	None
Carbon source	2% glucose (w/v)	None	None	2% glucose (w/v)
Add- back mix	Amino acids and nucleotides[b]†	Amino acids and nucleotides[b]	Nucleotides only[b]	Nucleotides only[b]

[a] Except for GAP1-GFP cultures, which used 87 mM proline.
[b] Except for protrophic strains, which omitted all add-back.

After 15 min, FM4-64 was removed by three washes in appropriate media at room temperature, and cells were incubated an additional 30 min at 30 °C. Sodium fluoride and sodium azide were added to 10 mM and cells were kept on ice until imaged. To assess FM4-64 recycling, cells grown to log phase or starved at different time points were pelleted and resuspended in appropriate media supplemented with 0.4 μg/ml FM4-64. After 15 min (for BY4741 background) or 8 min (for W303 background), cells were resuspended in ice-cold media and washed three times in ice-cold media. For cells labeled in replete media and then starved, the cells were washed with ice-cold media lacking glucose. Cells were kept on ice until assayed. For recycling monitored by loss of fluorescence intensity in Fig. 3*C* cells were monitored every 6 s at room temperature in a fluorometer as described (21). For recycling monitored by loss of fluorescence intensity in Fig. 3*D*, 30 μl of labeled cells was diluted to 1.5 OD_{600} with 100 μl of room temperature media in a room temperature opaque 96-well plate. Fluorescence emission at 680 nm was collected every 6 s from cells excited with 515 nm in a Spectramax M5e plate reader (Molecular Devices) at room temperature. For recycling monitored by an increase of FM4-64 in the media in Fig. 3*E*, 0.3 OD_{600} of labeled cells in 50 μl was transferred to a prewarmed microcentrifuge tube and incubated at 30 °C for 8 min. The supernatant was harvested by pelleting two times to remove any cells. CHAPs was added to 1% from a 20% stock solution in PBS, and fluorescence was monitored at 680 nm after excitation at 515 nm in a Spectramax M5e plate reader. To control for differences in FM4-64 accumulation between samples, background fluorescent signal from media without FM4-64 was first subtracted from all samples. The resultant background subtracted values were then normalized to the initial FM4-64 intensity of the cells assayed as in Fig. 3*D*.

Microscopy—For Figs. 1, 2*B*, 4, and 5, fluorescence microscopy was performed on an Eclipse TE2000-U (Nikon, Melville, NY) microscope with a 1.4 numerical aperture, 100× differential interference contrast oil immersion lens and the standard yEGFP and CFP/YFP/DsRed sets from Chroma (Rockingham, VT). Images were acquired with an ORCA ER-cooled CCD camera (Hamamatsu Photonics, Bridgewater, NY) with no binning, using MetaMorph (Molecular Devices) as the image acquisition software. For each cell, a 5-plane Z-stack was acquired with separation between adjacent planes set at 500 nm. For Figs. 3 and 5, images were acquired on a Nikon Ti-E inverted microscope equipped with a 100×, 1.4 numerical aperture oil immersion objective as described previously (22). Fluorescent samples were excited with the Lumencor light engine equipped with individual LEDs for GFP/YFP/mCherry excitation (Lumencor, Inc., Beaverton, OR). All of the filters were obtained from Chroma (Chroma Technology Corp., Bellows Falls, VT). Images were acquired with an Andor iXon camera (Andor Technology, South Windsor, CT) with a pixel size of 160 nm. For each cell, a 10-plane Z-stack was acquired with separation between adjacent planes set at 200 nm. The same integration time was used for all images of a labeled protein or fluorophore.

Intensity analysis of cell surface proteins was performed in ImageJ v1.43m (National Institutes of Health). For plasma membrane proteins with uniform plasma membrane localization, highest intensity measurements were collected from a 3-pixel-wide line drawn through a region of the plasma membrane away from the neck region from a central plane image. For proteins with nonuniform or punctate plasma membrane localization, highest intensity measurements were from a region with high intensity. Intensity measurements were collected for at least 20 different cells/sample. For intensity analysis of FM4-64 uptake, integrated cell intensity is reported from individual cells manually traced in ImageJ v1.43m.

For Fig. 3*A*, images were acquired using an Axiovert 200 inverted microscope (Carl Zeiss) equipped with a Cooke Sensicam (Cooke), an X-Cite 120 PC fluorescence illumination system, and a 100×, 1.4 numerical aperture Plan-Apochromat objective. All imaging was performed at room temperature, and identical acquisition parameters were used for all samples within an experiment. Image analysis was performed using ImageJ v1.41n. For all Mup1-GFP images, identical maximum and minimum intensity values were applied to each sample within a set of WT, 4Δ+Ent1 and 4Δ+ENTH1 cells.

Statistical Analysis—Except where noted, statistical significance was determined using a two-tailed Mann-Whitney *U* test for the null hypothesis that the medians were equal.

Preparation of Cell Lysates and Immunoblotting—For analysis of GFP-Atg8, whole cell extracts were performed as described previously (10). Following extractions, immunoblotting was performed as described previously. Monoclonal GFP antibody (B-2) was from Santa Cruz Biotechnology. Polyclonal antibody Adh1 antibody and fluorescent secondary antibodies were from Abcam and Invitrogen, respectively.

Amino Acid Analysis—Amino acid analysis was performed on cells grown to log phase or on cells grown to log phase, then washed three times into appropriate starvation media and grown for an additional 24 h. Amino acid extraction and analysis were performed as described previously (8).

Viability—Cell viability assays were performed on cells grown to log phase, then washed three times into appropriate starvation media. Cells were serially diluted and plated on YPD (1% yeast extract, 2% peptone, 2% glucose, 2% agar) plates or

incubated with aeration for 7 days, serially diluted, and plated. Plated cells were counted after 48 h.

RESULTS

Plasma Membrane to Vacuole Traffic Is Required for Cell Survival—Previous whole genome studies of glucose-starved cells suggested that autophagy is dispensable for survival during glucose starvation. However, several genes important for traffic to the vacuole are required for survival (7). We hypothesized that during glucose starvation, protein and lipid traffic to the vacuole may provide catabolic substrates necessary for cell viability. We assessed the contributions of endocytosis, endosomal membrane traffic, and autophagy to cell survival during glucose starvation by measuring the viability of strains lacking genes from each pathway. We measured the viability of wild-type cells, cells defective in endocytosis (*sla1*Δ and *rvs161*Δ), cells defective in vacuolar protein sorting (*vps4*Δ), cells defective in autophagy (*atg5*Δ), and cells defective in vacuolar proteolysis (*pep4*Δ) after 7 days of starvation (23–26). Wild-type and *atg5*Δ cells exhibited high viability after 7 days of starvation (Fig. 1*A*). In contrast, *sla1*Δ or *vps4*Δ cells were ~50% viable *pep4*Δ cells were 30% viable, and *rvs161*Δ cells were 15% viable (Fig. 1*A*). Together, these results indicate that endocytosis, vacuolar protein sorting, and vacuolar proteolytic function are important for cell survival during glucose starvation, whereas autophagy does not play an essential role.

We next monitored the fate of plasma membrane proteins during glucose starvation. We imaged cells expressing fluorescently tagged versions of several plasma membrane-localized proteins grown in the presence of 2% glucose and then starved for glucose for 30 min, 2 h, or 1 day (Fig. 1*B*). Of the 11 proteins tested, the cell surface levels of 9 proteins were significantly reduced within 2 h of starvation (Fig. 1, *B* and C). For these proteins, the cell surface levels decreased, and for many, punctate internal structures appeared within 30 min (Fig. 1*B*, *arrows*). Furthermore, after 2 h, the number or intensity of punctate internal structures was reduced whereas vacuolar fluorescence appeared or increased for many proteins (Fig. 1*B*, *arrowheads*). Notably, endocytosis seemed to occur for proteins unrelated to metabolism such as the pheromone receptor, Ste2, and the v-SNARE, Snc1. Thus, glucose starvation leads to the flux of numerous and diverse plasma membrane proteins to the vacuole.

We next tested whether clathrin-mediated endocytosis (CME) is required for the observed plasma membrane protein internalization. To do this, we used a previously established assay of clathrin-dependent endocytosis based on the clathrin adaptor-mediated internalization of Mup1-GFP, a methionine permease (15, 18). In control cells (WT and Δ4-pENT1), within 30 min of glucose starvation Mup1-GFP cell surface levels decreased, and Mup1-GFP appeared in internal structures (Fig. 2*A*). In contrast, in cells lacking CME due to deletion of multiple adaptors complemented by a plasmid encoding only a fragment of the adaptor Ent1 (Δ4-pENTH), Mup1-GFP remained at the cell surface for 2 h of glucose starvation and did not accumulate in internal structures. Similarly, in cells lacking *RVS161* more Tat2-GFP remained at the cell surface after 2 h of starvation than in wild-type cells (Fig. 2*B*). Together, these results demonstrate that the internalization of proteins in response to glucose starvation depends on CME.

Glucose Starvation Reduces Recycling from the Endosomes—The rerouting of plasma membrane proteins into the vacuole could result from increased rates of endocytosis, increased rates of traffic to the vacuole or reduced recycling of endocytosed proteins. We dissected the contribution of each of these mechanisms to the observed internalization of plasma membrane proteins upon glucose starvation using the dye FM4-64.

We first assessed changes in the rate of FM4-64 internalization. To monitor internalization, we incubated cells with FM4-64 for 2.5 min to allow internalization and then inhibited further traffic by placing the cells on ice and adding sodium azide and sodium fluoride to inhibit metabolic processes. Cells grown in replete media showed many small and medium sized foci of internalized FM4-64 consistent with many endocytic events and limited traffic to the early endosome (Fig. 3*A*). When cells were starved for glucose for 30 min prior to FM4-64 incubation, the internalization was less than half of that in the presence of glucose as monitored by total cell fluorescence and similar to the amount internalized by cells lacking *RVS161* (Fig. 3*A*, *chart*). This reduction in endocytosis rates in starved cells is consistent with the dependence of endocytosis on actin polymerization which requires ATP (27). These results show that the bulk internalization of plasma membrane proteins upon glucose starvation cannot be due to increased rates of endocytosis.

Next, we determined the rate of transport of internalized FM4-64 to the vacuole using a pulse-chase assay. We monitored FM4-64 traffic to the vacuole by labeling cells for a 15-min pulse followed by a 30-min chase. In the presence of glucose, FM4-64 was internalized and transported completely to the vacuole within 30 min (Fig. 3*B*, *arrows*). In contrast, when cells were starved for glucose for 30 min or 1 h prior to incubation with FM4-64, FM4-64 delivery to the vacuole was reduced as monitored by accumulation of FM4-64 in puncta and reduced numbers of cells with vacuolar staining (Fig. 3*B*, *arrows*). In contrast, cells lacking *RVS161* completed traffic to the vacuole. Thus, traffic to the vacuole is reduced in glucose-starved cells.

We noticed that cells starved for glucose for 30 min prior to FM4-64 labeling appeared to accumulate a high level of FM4-64 (Fig. 3*B*, *chart*). This suggests that at early time points after starvation, reduced endocytosis rates are counterbalanced with reduced recycling rates. Similarly, substantial FM4-64 accumulated in cells starved for 1 h prior to FM4-64 labeling despite the strong reduction in internalization rates at this time point. When combined with the lower rates of internalization, the substantial accumulation of FM4-64 indicates that glucose-starved cells have reduced rates of recycling.

Because the differences in whole cell intensity measurements in the pulse-chase experiment could be affected by the dramatically different morphology of the FM4-64 staining between starved and unstarved cells, we directly monitored changes in FM4-64 recycling from endosomes to the plasma membrane. We first incubated cells with FM4-64 for 15 min in the presence of glucose with no chase. When these cells were diluted into fresh media containing glucose, FM4-64 fluorescence rapidly decreased (Fig. 3*C*, *Replete*/*Replete*). This decrease reflects recycling of inter-

A.

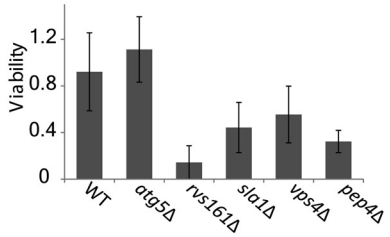

C.

Description	Gene	Change in Localization after 1 day
General amino acid transporter	Gap1	Internalization
Mating pheromone receptor	Ste2	Internalization
Ferro-oxidoreductase enzyme	Fet3	Internalization
Vitamin H transporter	Vht1	Internalization
Amino acid transporter	Tat1	Internalization
Low affinity glucose transporter	Hxt3	Internalization
Methionine transporter	Mup1	Internalization
Plasma membrane ATPase	Pma1	Partial Internalization
v-SNARE required	Snc1	Partial Internalization
Component of the eisosome	Sur7	Partial loss of cell surface localization
Bud site selection	Rax2	No response

B.

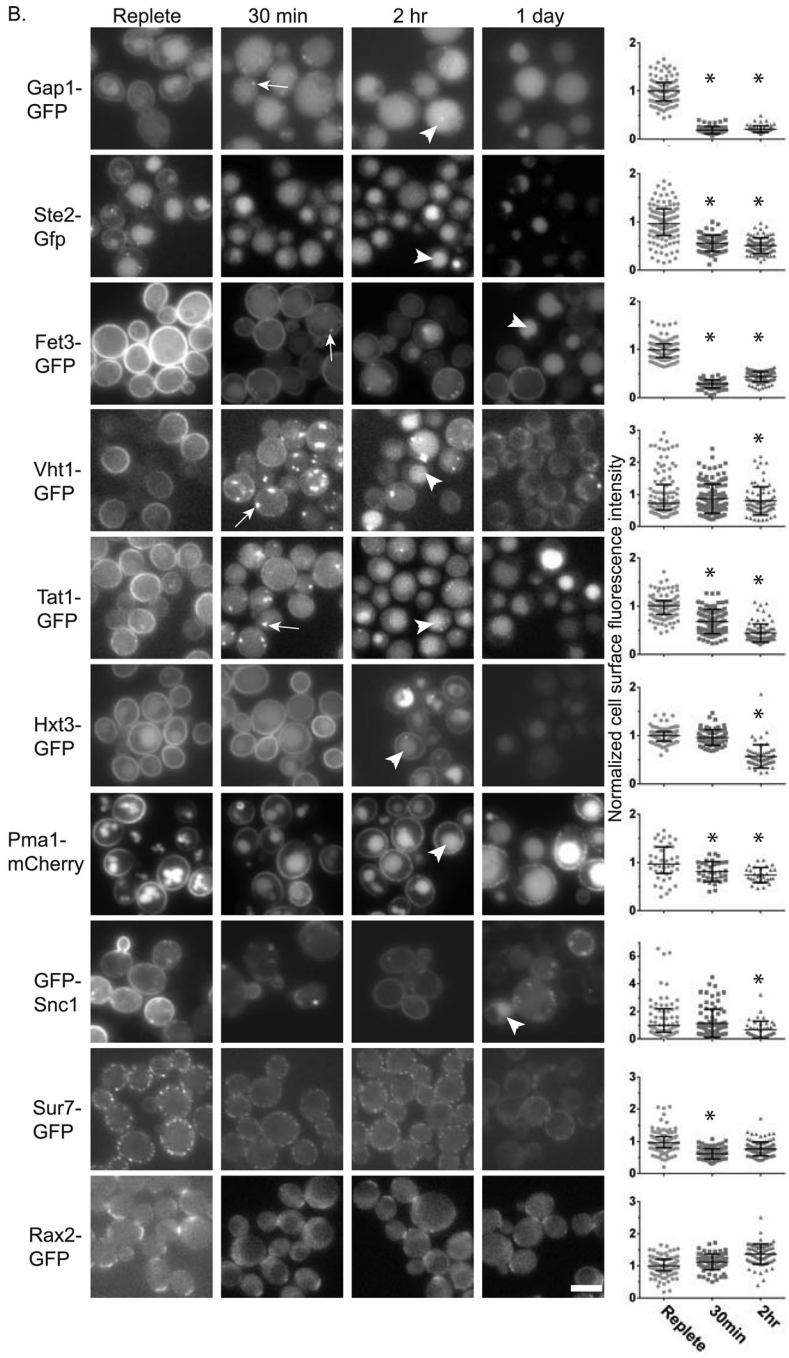

FIGURE 1. **Endocytosis and vacuolar protein sorting are required for survival during glucose starvation.** *A*, the indicated cells were grown to mid-log phase and starved for glucose. After 7 days, viability was assessed by colony-forming units. *Charts* indicate -fold change in colony-forming cells from initial unstarved replete cultures for three to six independent cultures. *B*, glucose starvation induces traffic of cell surface proteins to the vacuole. The indicated cells were imaged during log phase growth in replete media. Cells were washed into glucose starvation media and imaged at 30 min, 2 h, or after 1 day. *Arrows* indicate intracellular structures. *Arrowheads* indicate a vacuole as identified by transmitted light microscopy (data not shown). *Scale bar* is 5 μm. *Charts* show scatter dot plots of the cell surface intensity data normalized to median value for replete cells. The *horizontal lines* indicate the median and quartiles of the data. *, $p < 0.005$ for a difference between the replete and starved sample. *C*, cell surface proteins investigated and response to 1 day of glucose starvation are shown.

nalized FM4-64 to the cell surface (21). In contrast, when cells were diluted into media lacking glucose, FM4-64 was retained in the cell (Fig. 3*C*, *Replete*/*Starved*). Similar results were observed for cells starved for glucose for 30 min prior to labeling in the absence of glucose (Fig. 3*C*, *Starved*/*Starved*). We next tested how this decrease in recycling compared with cells with known defects in recycling. We used a previously characterized *rcy1*Δ and an isogenic wild-type strain (28). Starvation inhibited FM4-64 recycling more strongly than loss of *RCY1* (Fig. 3, *D* and *E*).Taken together, these results suggest that glucose starvation induces net flux from the cell surface to vacuole by inhibiting recycling of internalized cell surface proteins from the endosomes back to the plasma membrane.

Vacuolar Hydrolysis Inhibits Autophagy during Glucose Starvation—The net flux of proteins from the plasma membrane to the vacuole, when combined with the reduced viability

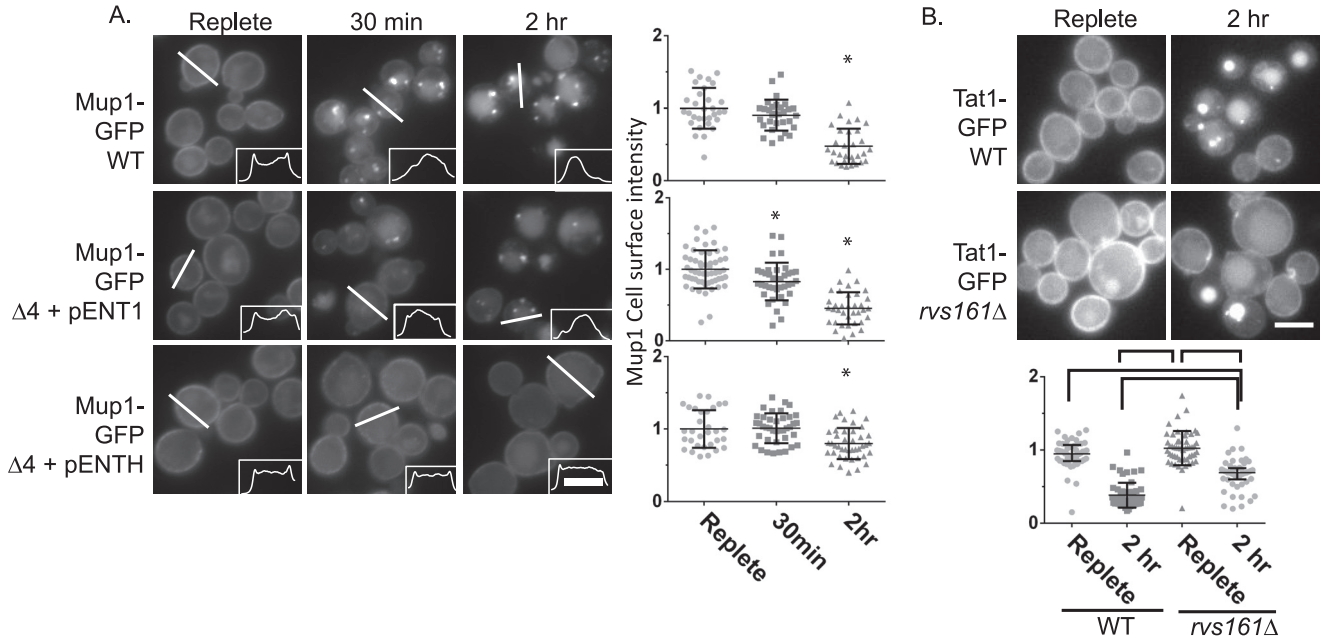

FIGURE 2. **CME is required for glucose starvation-induced endocytosis.** *A*, CME is important for redistribution of Mup1-GFP. *Left*, Mup1-GFP localization is shown in wild-type cells or cells lacking the four clathrin adaptors Ent1, Ent2, YAP1801, and Yap1802 (Δ4) and carrying either a plasmid encoding full-length Ent1 (*pENT1*), which complements the CME defect caused by loss of clathrin adaptors, or the ENTH domain of Ent1 (*pENTH*), which does not complements the CME defect. Cells were imaged after growth in replete media lacking methionine (to induce *MUP1* expression) or after starvation for glucose for 30 min or 2 h. *Insets* show line scans of regions indicated. *Right*, *charts* shown scatter dot plots of the data as in Fig. 1. *, $p < 0.005$ for a difference between replete and starved samples. *B*, CME is important for redistribution of Tat1-GFP. *Top*, the indicated cells were imaged after growth in replete media or after glucose starvation for 2 h. *Bottom*, *charts* show scatter box plots of the data as in Fig. 1 normalized to median intensity of WT cells in replete media. *Brackets* indicate pairs of samples for which $p < 0.005$.

of endocytic mutants during glucose starvation, suggests that endocytosis performs an essential role in adaption to starvation. In contrast, we found that autophagy is dispensable for survival (Fig. 1*A*). Although our finding is in accordance with previous reports that autophagy is not essential during glucose starvation, this dispensability is surprising because autophagy was reported to occur in glucose-starved yeast (7, 29). Therefore, we investigated whether autophagy was induced under our glucose starvation conditions. We monitored autophagy using GFP-Atg8 expressed from its endogenous promoter from a centromeric (low copy) plasmid. Atg8 covalently conjugates to the autophagosome membrane. Thus, autophagosome formation appears as GFP-Atg8 punctate localization. Upon autophagosome fusion with the vacuole, GFP-Atg8 is delivered into the vacuole where it is cleaved. Therefore, fusion of the autophagosome with the vacuole causes vacuolar localization of GFP and appearance of free GFP, as detected by immunoblot analysis (30). Furthermore, this system allows us to investigate the normal transcriptional response of *ATG8* during starvation. In response to 16 h of glucose starvation, punctate GFP-Atg8 structures accumulated (Fig. 4*A*). However, little Atg8 was delivered to the vacuole as monitored by fluorescence microscopy or by immunoblot analysis (Fig. 4, *A* and *B*). We found similar results with a quantitative assay of autophagy that measures delivery of a cytosolic form of the phosphatase Pho8 (Pho8Δ60) to the vacuole (Fig. 4*C*) (31). These results suggest that glucose starvation does not induce high levels of autophagy, contrary to previous reports.

The disagreement between our results and previous reports can be explained by a specific experimental design feature used previously (29). The prior study used cells lacking vacuolar hydrolysis to accumulate autophagic bodies in the vacuole. During glucose starvation, vacuolar hydrolysis should release amino acids and lipids, which could regulate autophagy (32, 33). Amino acids inhibit autophagy through activating TORC1 (34). Similarly, energy derived from lipids can inhibit autophagy by converting ADP to ATP, thereby inhibiting AMPK, a potent activator of autophagy (5, 35). Therefore, we hypothesized that, in the prior study, autophagy was induced inadvertently upon glucose starvation because the normal regulation of pathways like TORC1 and AMPK by protein and lipid hydrolysis in the vacuole was disrupted.

To test this possibility, we monitored autophagy in cells lacking the primary vacuolar hydrolase Pep4. In *pep4*Δ cells, GFP-Atg8 puncta accumulated after 16 h of glucose starvation, indicating autophagy onset (Fig. 4*D*). Importantly, unlike puncta in wild-type cells, many puncta in the *pep4*Δ cells were in the vacuole as assessed by transmitted light microscopy (Fig. 4*D*). This suggests that in *pep4*Δ cells, autophagosomes fuse with the vacuole; however, the autophagic bodies do not break down because Pep4 is required to activate vacuolar lipases that hydrolyze the membrane components of the autophagic bodies (36). As a further test, we treated wild-type cells with the cell-permeant protease inhibitor PMSF during the course of glucose starvation. Cells treated with PMSF induced autophagy as monitored by GFP fluorescence in the vacuole (Fig. 4*E*). Together, these results suggest that the products of vacuolar hydrolysis prevent autophagy upon glucose starvation.

To further test the hypothesis that vacuolar hydrolysis inhibits autophagy, we examined autophagy in cells lacking *VPH1*

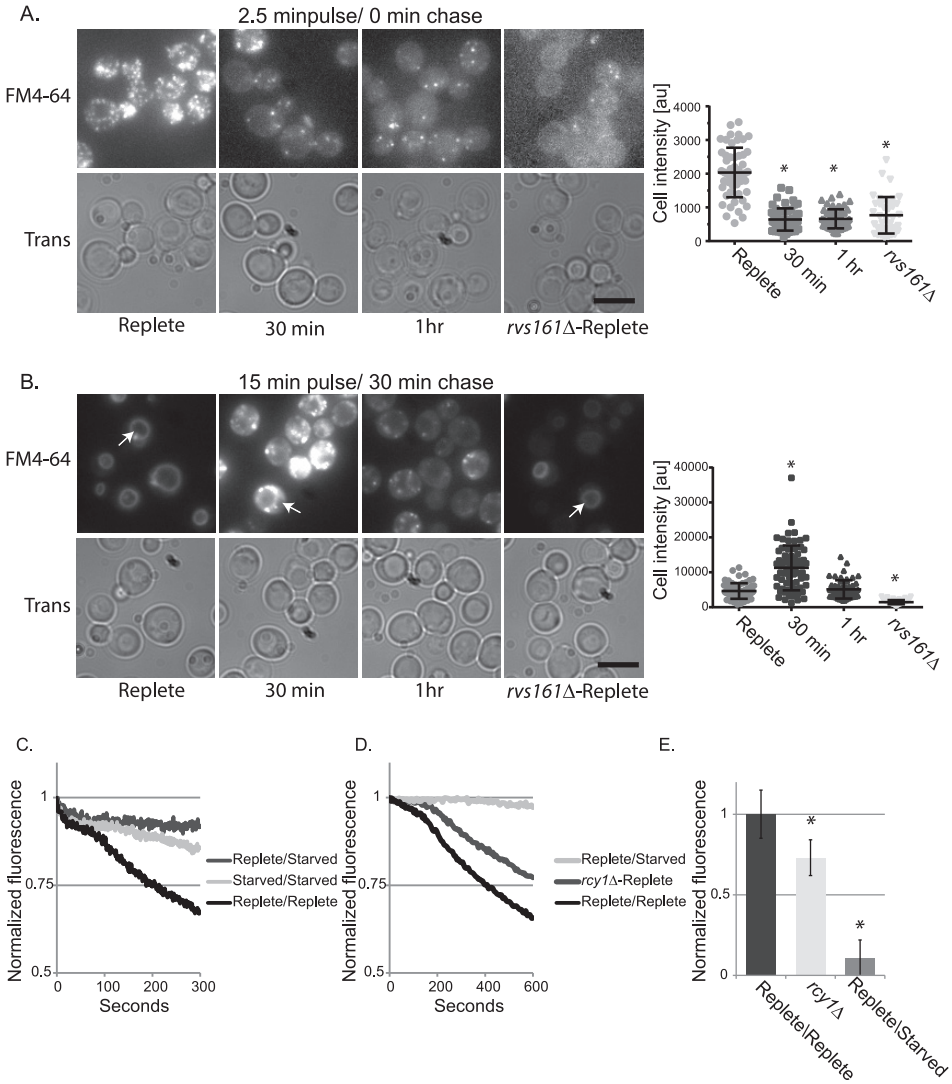

FIGURE 3. **Glucose starvation alters FM4-64 traffic.** *A*, internalization of FM4-64 was monitored in wild-type cells treated with FM4-64 for 2.5 min in replete media or in glucose starvation media after starvation for indicated time points or in *rvs161*Δ cells in replete media (*far right*). *Lower panels* show transmitted light images (*Trans*). *Charts* show scatter box plots of whole cell intensity data in arbitrary units. *, $p < 0.005$ for a difference from wild-replete. *B*, FM4-64 delivery to the vacuole, and whole cell accumulation was monitored by pulse-chase analysis in cells grown in replete media or glucose-starved for indicated time points or in *rvs161*Δ cells in replete media (*far right*). *Arrow* indicates vacuolar labeling. *Charts* show scatter box plots of whole cell intensity in arbitrary units. *, $p < 0.005$ for a difference from wild-type replete. *C*, FM4-64 recycling was monitored in cells that were labeled in replete media and then washed into replete media (*Replete*/*Replete*) or glucose starvation media (*Replete*/*Starved*) or in cells that were starved for glucose for 30 min prior to labeling and then washed into glucose starvation media (*Starved*/*Starved*). *Chart* shows data normalized to initial sample fluorescence averages of three independent experiments. S.D. were <6% of the averaged value at each time point; for clarity, S.D. are not shown. *D*, FM4-64 recycling was monitored in wild-type or *rcy1*Δ W303 cells as in *C*. *Charts* show representative data. *E*, FM4-64 recycling was monitored as FM4-64 present in culture media from cells in *D* after 8 min of recycling at 30 °C. *Chart* shows average fluorescence for four samples.*, $p < 0.05$ determined by a two-tailed Student's *t* test for a difference from wild-type replete.

and *VPS4*. *VPH1* encodes a vacuolar-specific component of the V-ATPase required for acidification of the vacuole and maximal hydrolytic activity (37–39). *VPS4* is involved in sorting of proteins into the lumen of the vacuole and through this role may be required for maximal proteolytic activity (40). In cells lacking *VPH1* or *VPS4*, autophagy was higher as monitored by fluorescence microscopy (Fig. 4*F*). In immunoblot analysis, the levels of both full-length GFP-Atg8 and free GFP were higher in glucose-starved *vph1*Δ and *vps4*Δ cells than in wild-type cells (Fig. 4*B*). The elevation of both full-length and cleaved GFP-Atg8 is likely caused by the combined effects of elevated transcription from the *ATG8* promoter due to transcriptional activation of autophagy, and enhanced delivery of GFP-Atg8 to the vacuole but decreased proteolysis in the vacuole (41). These results further suggest that hydrolytic activity in the vacuole prevents autophagy during glucose starvation. They also explain the discrepancy between our observations and previous reports based in cells with protease-deficient vacuoles.

Although glucose starvation did not induce high levels of autophagy as detected by delivery of GFP-Atg8 or Pho8Δ60 to the vacuole, glucose-starved cells frequently contained more GFP-Atg8 puncta than cells in replete media. This suggests that although autophagy is initiated during glucose starvation, glucose starvation does not provide all of the signals required to complete autophagy or that glucose starvation produces a signal that inhibits autophagy completion. To test these possibilities, we asked whether glucose starvation influenced autophagy initiated by nitrogen starvation. Nitrogen starvation is a potent activa-

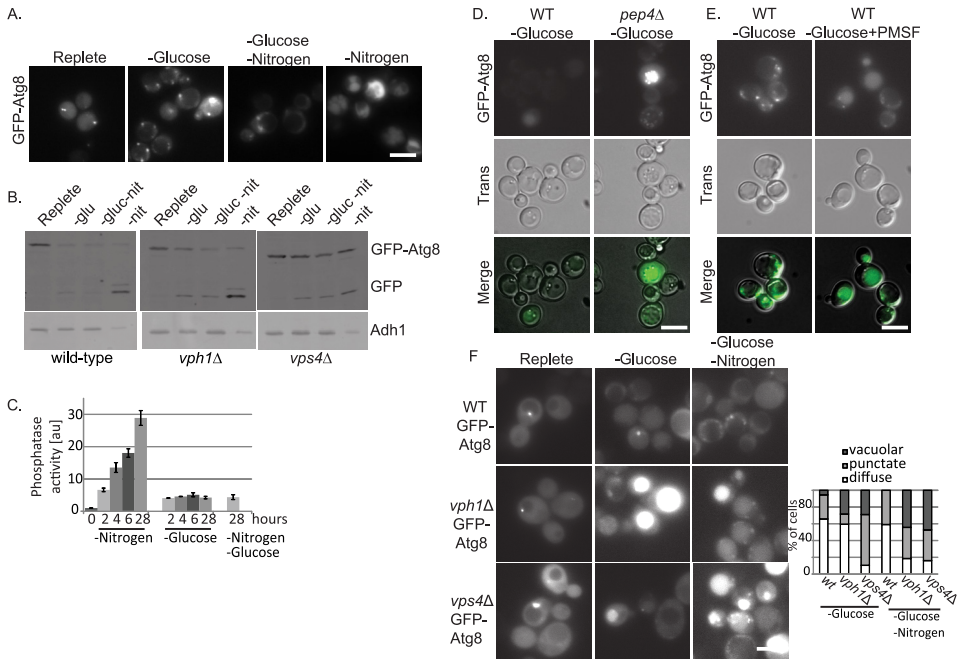

FIGURE 4. **Vacuolar proteolysis inhibits autophagy in glucose-starved cells.** *A*, wild-type cells transformed with a plasmid expressing *GFP-ATG8* were grown in replete media lacking uracil and imaged. Portions of the remaining sample were washed into the indicated starvation media. Starved cells were imaged after 16 h of treatment. *B*, cell lysates were taken from samples described in *A* and *F* and subjected to immunoblot analysis for GFP or the load control Adh1. *C*, autophagy was monitored by Pho8Δ60 assay in cells grown in replete media and starved for indicated nutrients and time points. *D* and *E*, the indicated cells were treated as in *A*. For cells treated with PMSF, PMSF was added after the final wash with glucose starvation media. *Middle panel* shows transmitted (*Trans*) light image of cells. *F*, wild-type, *vph1*Δ, or *vps4*Δ cells treated and imaged as in *A*. *Chart* shows percentage of cells categorized as containing diffuse cytosolic, punctate cytosolic, or vacuolar GFP-Atg8 localization

tor of autophagy. We starved cells for nitrogen only or both glucose and nitrogen at the same time. In cells starved for nitrogen, autophagy completed as monitored by all three assays used (Fig. 4, *A*–*C*). In contrast, when cells were starved for both glucose and nitrogen concurrently, few cells showed evidence of completed autophagy by all three assays used (Fig. 4, *A*–*C*). However, in *vph1*Δ and *vps4*Δ cells autophagy completed as monitored by GFP fluorescence in the vacuole and the accumulation of free GFP (Fig. 4, *B* and *F*). Together, these results indicate that glucose starvation actively inhibits autophagy and that the mechanism of inhibition requires efficient vacuolar hydrolysis.

We tested whether the requirement for vacuolar proteolysis was due to the use of auxotrophic strains. We found that in a prototrophic strain GFP-Atg8 was not delivered to the vacuole during starvation for glucose or glucose and nitrogen (Fig. 5*A*). Furthermore, in a prototrophic strain lacking *PEP4* or treated with PMSF, GFP-Atg8 was delivered to the vacuole during glucose starvation (Fig. 5*B*). To determine when GFP accumulation initiated in the vacuole in the prototrophic proteolytic-deficient strains, we monitored GFP-Atg8 accumulation after 1, 3, or 23 h of glucose starvation (Fig. 5*B*). Prior to glucose starvation cells lacking *PEP4* had more GFP detected in the vacuole than wild-type cells. The GFP detected was primarily in the form of highly motile puncta. After 1 h of starvation, more than half of the *pep4*Δ cells had GFP present in the vacuole. Starvation for longer periods did not increase the number of cells with GFP in the vacuole, but it did increase the number of puncta. In cells treated with PMSF, after 1 h of starvation the number of cells with vacuolar staining was similar to that of cells not treated with PMSF. However, by 3 h, nearly 40% of PMSF-treated cells had GFP in the vacuole, and by 23 h >70% of cells had GFP in the vacuole. Thus, even in cells capable of making all amino acids, glucose starvation does not induce autophagy, and vacuolar hydrolysis inhibits autophagy.

The vacuole is the hydrolytic end point for numerous pathways including multiple forms of autophagy, membrane traffic from the endosomes, and membrane traffic from the Golgi. We tested the contribution of endocytosis to the inhibition of autophagy. We found that in cells lacking *SLA1* or *RVS161*, GFP-Atg8 was not delivered to the vacuole after 16 h of starvation for glucose or glucose and nitrogen (Fig. 5*C*). This suggests that endocytosis does not contribute to the inhibition of autophagy.

Glucose Starvation Elevates Free Amino Acid Levels via Vacuolar Hydrolysis—Because amino acids are potent inhibitors of autophagy, we hypothesized that glucose starvation may inhibit autophagy through the production of amino acids via vacuolar hydrolysis. Accordingly, a previous metabolomics study demonstrated that free amino acids increase in glucose-starved cells (42). To test whether vacuolar hydrolysis was important for this increase, we monitored a subset of free amino acid levels in wild-type, *pep4*Δ, and *vps4*Δ cells. Of the 17 amino acids monitored, the levels of 8 rose >2-fold in response to glucose starvation in wild-type cells (Fig. 6*A* and supplemental Data Base). A notable exception is methionine, which decreased to less than half of the levels seen in replete conditions. In *pep4*Δ or *vps4*Δ cells, the increases of amino acids were strongly reduced for 6 of the 8 amino acids: valine, isoleucine, tyrosine, phenylalanine, histidine, and arginine, but not lysine or cysteic acid (Fig. 6*A*). We also found that many free amino acids levels rose

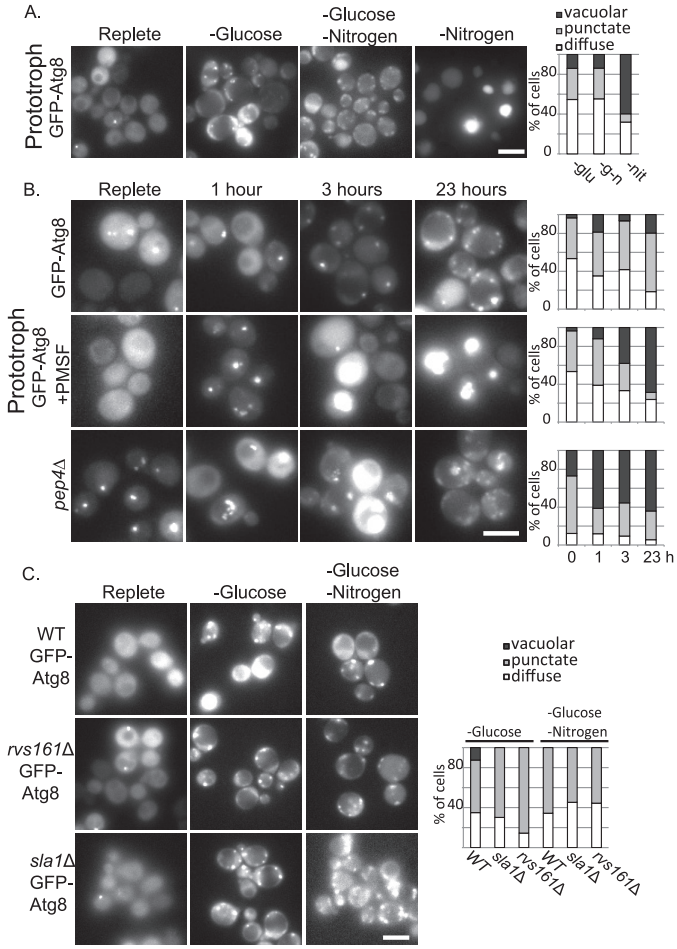

FIGURE 5. **Vacuolar proteolysis inhibits autophagy in prototrophic glucose-starved cells.** *A*, wild-type cells auxotrophic for only *URA* (LWY 114) were transformed with a plasmid expressing *GFP-ATG8* and the uracil auxotrophic marker, grown in replete media without any add-back mix and starved as in Fig. 4. *B*, wild-type or *pep4*Δ cells auxotrophic for only *URA* (DLY434 and 432) were treated as in *A* and imaged at indicated time points after starvation for glucose. For cells treated with PMSF, PMSF was added after the final wash with glucose starvation media. *C*, defects in endocytosis do not increase autophagy response to glucose starvation. Auxotrophic wild-type, *rvs161*Δ, or *sla1*Δ cells transformed with a plasmid expressing *GFP-ATG8* were treated as in Fig. 4*A*. Starved cells were imaged after 16 h of treatment. Charts show the percentage of cells in the sample categorized as containing diffuse cytosolic, punctate cytosolic, or vacuolar GFP-Atg8 localization. *Scale bars* are 5 μm.

in cells starved for both glucose and nitrogen (Fig. 6*A*). Notably, many amino acids rose to higher levels in cells starved for both glucose and nitrogen than for cells starved for glucose alone. Furthermore, we found that in *pep4*Δ or *vps4*Δ cells starved for both glucose and nitrogen the amino acid levels were even lower than in glucose starvation alone (Fig. 6*A*). This observation suggests the mechanism by which glucose starvation inhibits autophagy in the presence of nitrogen starvation; when cells are starved for both glucose and nitrogen, amino acids released from vacuolar hydrolysis inhibits autophagy.

We next tested the contribution of endocytosis to the release of amino acids. We found that inhibiting endocytosis caused an intermediate effect on amino acid levels. Glucose-starved *rvs161*Δ cells had lower levels of glutamine, valine, alanine, isoleucine, and threonine than glucose-starved wild-type cells. However, in glucose- and nitrogen-starved cells most amino acids accumulated in *rvs161*Δ at levels similar to wild-type cells. Overall, these results show that endocytosis only contributes partially to release of amino acids in glucose-starved cells.

Because TORC1 is a potent inhibitor of autophagy that is activated by amino acids, we tested whether TORC1 was required to inhibit autophagy in glucose-starved cells (43–45). We first glucose-starved cells for several hours then inhibited TORC1 with rapamycin for several hours and assessed autophagy. In contrast to untreated cells, rapamycin-treated cells completed autophagy as assessed by three assays (Fig. 6, *B–D*). These results indicate that TORC1 is normally active in glucose-starved cells, and its activity inhibits autophagy during glucose starvation.

DISCUSSION

Our results reveal a suite of cell behaviors induced by glucose starvation, which includes reduced recycling, increased free amino acids, and inhibited autophagy. We proposed that that these three behaviors are mechanistically linked (Fig. 6*E*). In this scenario, inhibited recycling is the crucial step. It is initiated by the acute drop in ATP levels caused by glucose starvation. Inhibited recycling drives the net flux of proteins to the vacuole by preventing endocytosed proteins from trafficking back to the plasma membrane. Although low ATP also reduces bulk endocytosis rates, endocytosis rates remain high enough to drive substantial internalization of proteins and FM4-64. The increase in free amino acids and subsequent inhibition of autophagy derive from the flux of proteins from the plasma membrane and elsewhere to the vacuole. Thus, these three cellular responses are likely a single mechanistic response to glucose starvation. However, several key questions remain.

It is unclear why recycling is strongly inhibited by glucose starvation whereas endocytosis seems less sensitive. Glucose starvation induces an acute drop in ATP. This reduces the levels of phosphatidylinositol 4-phosphate at the *trans*-Golgi network and endosomes (3, 46, 47). Furthermore, glucose starvation causes ADP-ribosylation factor (Arf) to delocalize from endosomes (3). Phosphatidylinositol 4-phosphate and Arf recruit many proteins implicated in endosomal recycling. Failure to recruit these endosomal proteins when ATP levels are low could cause reduced recycling (48–53). In addition to these known changes, unexplored mechanisms such as changes in ubiquitination/deubiquitination enzyme activities, alterations in endosomal or vacuolar pH, changes in activities of lipid flippases, or any combination of these factors could be the mechanism(s) of inhibited recycling during glucose starvation (54–57). Regardless of the mechanism, inhibited recycling seems to be a conserved response to ATP depletion. In metazoan cells, ATP depletion causes the internalization of proteins that seem unrelated to energy (58–60). Furthermore, similar to the behavior observed in glucose-starved yeast cells, this internalization is a result of reduced recycling (58). Thus, the overall behavior likely reflects an ancient response to energy depletion.

How the cell selects proteins for endocytosis during glucose starvation is unclear. Diverse proteins undergo endocytosis upon glucose starvation. Because cells defective in endocytosis die during glucose starvation, endocytosis performs an essential function during glucose starvation. Endocytosis may be

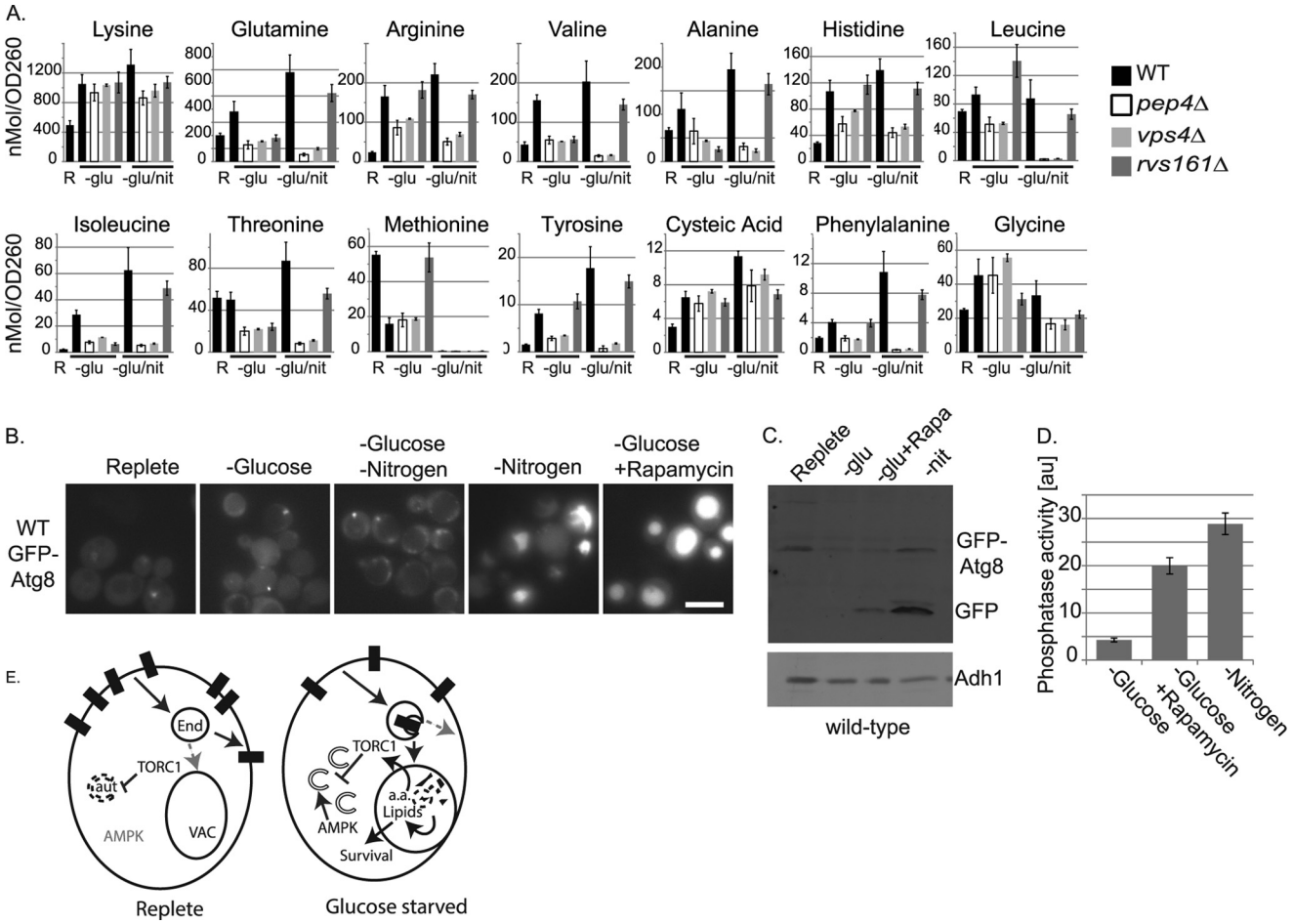

FIGURE 6. **Vacuolar hydrolysis elevates amino acid levels and inhibits autophagy through TORC1.** *A*, free amino acids were extracted from the indicated cells grown to mid-log phase (*R*) or starved for glucose (−*glu*) or for glucose and nitrogen (−*glu/nit*) for 24 h. *Charts* show a subset of the monitored amino acids. *B*, autophagy was monitored as in Fig. 4. For cells treated with rapamycin, cells were starved for 16 h and then treated with 200 nM rapamycin. Rapamycin-treated cells and untreated controls were imaged at 24 h. *C*, cell lysates were taken from samples in *B* and subjected to immunoblot analysis for GFP or the load control Adh1. *D*, autophagy was monitored with phosphatase activity as in Fig. 4. For rapamycin-treated cells, cells were starved for glucose for 10 h and then treated with rapamycin. Assay was performed at 28 h. *E*, model of cellular responses to glucose starvation. In replete cells, autophagy (*aut*) is inhibited by the activity of TORC1. Many cell surface proteins are endocytosed to the endosomes (*end*) but recycle back to the cell surface and do not traffic to the vacuole (*vac*). During glucose starvation, endocytosis continues at reduced rates while recycling stops. This leads to cell survival and, potentially, accumulation of amino acids as described under "Discussion." Increased amino acids activate TORC1, which counteracts the activity of AMPK leading to the initiation but not completion of autophagy.

required to remove deleterious proteins from the cell surface. For example, ATP-dependent transporters might deplete cellular ATP to lethal levels if left at the plasma membrane. An additional, but not mutually exclusive, model is that endocytosis acts as an alternative to autophagy and allows the cell to catabolize the lipids and amino acids from the plasma membrane as resources for survival. Understanding how proteins are selected for endocytosis may help explain the requirement for endocytosis.

The model that endocytosis provides catabolic substrates suggests a novel survival mechanism that is tailored to meet the specific cellular needs during acute energy starvation. By rerouting endocytic traffic to the vacuole, the cell can hydrolyze the lipid content of the plasma membrane. Because lipids are a rich source of energy, this mechanism will resupply the cell with energy. In contrast, autophagy is not known to access this pool of lipids. Furthermore, autophagy can promote the hydrolysis of peroxisomes and mitochondria (61). The degradation of these organelles is counterproductive in energy stress because these organelles are required to generate energy through β-oxidation and subsequent respiration. The risk of destroying these organelles may explain why, when faced with both amino acid and glucose starvation, the cell opts to inhibit autophagy.

Indeed, our results suggest that the down-regulation of recycling and inhibition of autophagy could be linked. Our results demonstrate that vacuolar function inhibits autophagy. This inhibition depends at least in part on TORC1, suggesting that the accumulation of amino acids in glucose-starved cells inhibits autophagy. An attractive model is that the accumulated amino acids derive from endocytosed proteins; however, cells lacking *RVS161* or *SLA1* inhibit autophagy as well as wild-type cells. Interestingly, deletion of *RVS161* reduces the accumulation of several amino acids, but not the key autophagy regulator leucine (45). Thus, endocytosis likely contributes to the accumulated amino acids but is not essential for the key autophagy-regulating amino acids. Additional routes to the vacuole may thus contribute to accumulated amino acids during glucose starvation. Possible routes include microautophagy, clathrin-

independent endocytosis, and reduced recycling to biosynthetic organelles leading to consumption of proteins and lipids from such organelles as the Golgi, endoplasmic reticulum, and endosomes. Furthermore, amino acid accumulation will also be influenced by the release of free amino acids from proteasomal degradation, the import from extracellular supplies, and the consumption of the free amino acids in the form of protein biosynthesis or other metabolic uses. Indeed, the accumulation of amino acids in cells starved for glucose could be caused by overall reduced protein synthesis due to low methionine in these cells (Fig. 5*A*). Thus, the impact of mutations on amino acid accumulation is difficult to interpret. Regardless of the source of the free amino acids accumulating in wild-type cells, our results provide strong evidence that vacuolar hydrolysis of lipids or proteins activates TORC1 and inhibits autophagy in glucose-starved cells.

The finding that vacuolar hydrolysis inhibits autophagy and activates TORC1 contributes to a growing literature about the importance of lysosomal function for correct regulation of these processes (44, 62). Indeed, there is growing concern about the use of lysosomal inhibitors in autophagy research (63, 64). Such inhibitors are commonly used to accumulate intermediates of macroautophagy to facilitate their detection (65). However, such inhibitors will also prevent the normal release of many metabolites. In addition to lipids and amino acids, vacuolar hydrolysis in yeast is important for the mobilization of phosphate and storage carbohydrates (66, 67). By preventing the release of these resources, lysosomal inhibitors may increase the strength of a normal starvation response or may even activate a starvation response that would not normally occur. Thus, the finding reported here that inhibiting vacuolar hydrolysis in glucose-starved cells promotes autophagy provides additional evidence about the possible confounding impact of lysosomal inhibitors on experimental outcomes.

Acknowledgments—We thank Drs. D. Winge for help with amino acid analysis; A. Tripathy for help with fluorometry; K. S. Bloom and A. P. Joglekar for use of fluorescence microscopes; D. J. Klionsky, L. S. Weisman, P. K. Herman, N. Segev, and Jeffery Gerst for reagents and advice; and A. M. Jones, A. P. Joglekar, and three anonymous reviewers for improving the manuscript.

REFERENCES

1. Vander Heiden, M. G., Cantley, L. C., and Thompson, C. B. (2009) Understanding the Warburg effect: the metabolic requirements of cell proliferation. *Science* **324,** 1029–1033
2. Ashe, M. P., De Long, S. K., and Sachs, A. B. (2000) Glucose depletion rapidly inhibits translation initiation in yeast. *Mol. Biol. Cell* **11,** 833–848
3. Aoh, Q. L., Hung, C. W., and Duncan, M. C. (2013) Energy metabolism regulates clathrin adaptors at the trans-Golgi network and endosomes. *Mol. Biol. Cell* **24,** 832–847
4. Singh, R., and Cuervo, A. M. (2011) Autophagy in the cellular energetic balance. *Cell Metab.* **13,** 495–504
5. Stephan, J. S., and Herman, P. K. (2006) The regulation of autophagy in eukaryotic cells: do all roads pass through Atg1? *Autophagy* **2,** 146–148
6. Thevelein, J. M., and de Winde, J. H. (1999) Novel sensing mechanisms and targets for the cAMP-protein kinase A pathway in the yeast *Saccharomyces cerevisiae*. *Mol. Microbiol.* **33,** 904–918
7. Klosinska, M. M., Crutchfield, C. A., Bradley, P. H., Rabinowitz, J. D., and Broach, J. R. (2011) Yeast cells can access distinct quiescent states. *Genes Dev.* **25,** 336–349
8. Jones, C. B., Ott, E. M., Keener, J. M., Curtiss, M., Sandrin, V., and Babst, M. (2012) Regulation of membrane protein degradation by starvation-response pathways. *Traffic* **13,** 468–482
9. Uesono, Y., Ashe, M. P., and Toh-E, A. (2004) Simultaneous yet independent regulation of actin cytoskeletal organization and translation initiation by glucose in Saccharomyces cerevisiae. *Mol. Biol. Cell* **15,** 1544–1556
10. Aoh, Q. L., Graves, L. M., and Duncan, M. C. (2011) Glucose regulates clathrin adaptors at the TGN and endosomes. *Mol. Biol. Cell* **22,** 3671–3683
11. Beck, T., Schmidt, A., and Hall, M. N. (1999) Starvation induces vacuolar targeting and degradation of the tryptophan permease in yeast. *J. Cell Biol.* **146,** 1227–1238
12. Volland, C., Urban-Grimal, D., Géraud, G., and Haguenauer-Tsapis, R. (1994) Endocytosis and degradation of the yeast uracil permease under adverse conditions. *J. Biol. Chem.* **269,** 9833–9841
13. Kamada, Y., Funakoshi, T., Shintani, T., Nagano, K., Ohsumi, M., and Ohsumi, Y. (2000) Tor-mediated induction of autophagy via an Apg1 protein kinase complex. *J. Cell Biol.* **150,** 1507–1513
14. Maldonado-Báez, L., Dores, M. R., Perkins, E. M., Drivas, T. G., Hicke, L., and Wendland, B. (2008) Interaction between Epsin/Yap180 adaptors and the scaffolds Ede1/Pan1 is required for endocytosis. *Mol. Biol. Cell* **19,** 2936–2948
15. Prosser, D. C., Whitworth, K., and Wendland, B. (2010) Quantitative analysis of endocytosis with cytoplasmic pHluorin chimeras. *Traffic* **11,** 1141–1150
16. Winston, F., Dollard, C., and Ricupero-Hovasse, S. L. (1995) Construction of a set of convenient *Saccharomyces cerevisiae* strains that are isogenic to S288C. *Yeast* **11,** 53–55
17. Longtine, M. S., McKenzie, A., 3rd, Demarini, D. J., Shah, N. G., Wach, A., Brachat, A., Philippsen, P., and Pringle, J. R. (1998) Additional modules for versatile and economical PCR-based gene deletion and modification in *Saccharomyces cerevisiae*. *Yeast* **14,** 953–961
18. Prosser, D. C., Drivas, T. G., Maldonado-Báez, L., and Wendland, B. (2011) Existence of a novel clathrin-independent endocytic pathway in yeast that depends on Rho1 and formin. *J. Cell Biol.* **195,** 657–671
19. Suzuki, K., Kirisako, T., Kamada, Y., Mizushima, N., Noda, T., and Ohsumi, Y. (2001) The pre-autophagosomal structure organized by concerted functions of APG genes is essential for autophagosome formation. *EMBO J.* **20,** 5971–5981
20. Kama, R., Robinson, M., and Gerst, J. E. (2007) Btn2, a Hook1 ortholog and potential Batten disease-related protein, mediates late endosome-Golgi protein sorting in yeast. *Mol. Cell. Biol.* **27,** 605–621
21. Wiederkehr, A., Avaro, S., Prescianotto-Baschong, C., Haguenauer-Tsapis, R., and Riezman, H. (2000) The F-box protein Rcy1p is involved in endocytic membrane traffic and recycling out of an early endosome in *Saccharomyces cerevisiae*. *J. Cell Biol.* **149,** 397–410
22. Aravamudhan, P., Felzer-Kim, I., and Joglekar, A. P. (2013) The budding yeast point centromere associates with two Cse4 molecules during mitosis. *Curr. Biol.* **23,** 770–774
23. Babst, M., Sato, T. K., Banta, L. M., and Emr, S. D. (1997) Endosomal transport function in yeast requires a novel AAA-type ATPase, Vps4p. *EMBO J.* **16,** 1820–1831
24. Ammerer, G., Hunter, C. P., Rothman, J. H., Saari, G. C., Valls, L. A., and Stevens, T. H. (1986) *PEP4* gene of *Saccharomyces cerevisiae* encodes proteinase A, a vacuolar enzyme required for processing of vacuolar precursors. *Mol. Cell. Biol.* **6,** 2490–2499
25. Woolford, C. A., Daniels, L. B., Park, F. J., Jones, E. W., Van Arsdell, J. N., and Innis, M. A. (1986) The *PEP4* gene encodes an aspartyl protease implicated in the posttranslational regulation of *Saccharomyces cerevisiae* vacuolar hydrolases. *Mol. Cell. Biol.* **6,** 2500–2510
26. Kametaka, S., Matsuura, A., Wada, Y., and Ohsumi, Y. (1996) Structural and functional analyses of *APG5*, a gene involved in autophagy in yeast. *Gene* **178,** 139–143
27. Belmont, L. D., and Drubin, D. G. (1998) The yeast V159N actin mutant reveals roles for actin dynamics *in vivo*. *J. Cell Biol.* **142,** 1289–1299
28. Chen, S. H., Chen, S., Tokarev, A. A., Liu, F., Jedd, G., and Segev, N. (2005) Ypt31/32 GTPases and their novel F-box effector protein Rcy1 regulate

protein recycling. *Mol. Biol. Cell* **16,** 178–192
29. Takeshige, K., Baba, M., Tsuboi, S., Noda, T., and Ohsumi, Y. (1992) Autophagy in yeast demonstrated with proteinase-deficient mutants and conditions for its induction. *J. Cell Biol.* **119,** 301–311
30. Klionsky, D. J. (2011) For the last time, it is GFP-Atg8, not Atg8-GFP (and the same goes for LC3). *Autophagy* **7,** 1093–1094
31. Noda, T., and Klionsky, D. J. (2008) The quantitative Pho8Δ60 assay of nonspecific autophagy. *Methods Enzymol.* **451,** 33–42
32. Yorimitsu, T., Zaman, S., Broach, J. R., and Klionsky, D. J. (2007) Protein kinase A and Sch9 cooperatively regulate induction of autophagy in *Saccharomyces cerevisiae*. *Mol. Biol. Cell* **18,** 4180–4189
33. Stephan, J. S., Yeh, Y. Y., Ramachandran, V., Deminoff, S. J., and Herman, P. K. (2009) The Tor and PKA signaling pathways independently target the Atg1/Atg13 protein kinase complex to control autophagy. *Proc. Natl. Acad. Sci. U.S.A.* **106,** 17049–17054
34. Loewith, R. (2011) A brief history of TOR. *Biochem. Soc. Trans.* **39,** 437–442
35. Mayer, F. V., Heath, R., Underwood, E., Sanders, M. J., Carmena, D., McCartney, R. R., Leiper, F. C., Xiao, B., Jing, C., Walker, P. A., Haire, L. F., Ogrodowicz, R., Martin, S. R., Schmidt, M. C., Gamblin, S. J., and Carling, D. (2011) ADP regulates SNF1, the *Saccharomyces cerevisiae* homolog of AMP-activated protein kinase. *Cell Metab.* **14,** 707–714
36. Teter, S. A., Eggerton, K. P., Scott, S. V., Kim, J., Fischer, A. M., and Klionsky, D. J. (2001) Degradation of lipid vesicles in the yeast vacuole requires function of Cvt17, a putative lipase. *J. Biol. Chem.* **276,** 2083–2087
37. Manolson, M. F., Wu, B., Proteau, D., Taillon, B. E., Roberts, B. T., Hoyt, M. A., and Jones, E. W. (1994) *STV1* gene encodes functional homologue of 95-kDa yeast vacuolar H^+-ATPase subunit Vph1p. *J. Biol. Chem.* **269,** 14064–14074
38. Kawasaki-Nishi, S., Bowers, K., Nishi, T., Forgac, M., and Stevens, T. H. (2001) The amino-terminal domain of the vacuolar proton-translocating ATPase a subunit controls targeting and *in vivo* dissociation, and the carboxyl-terminal domain affects coupling of proton transport and ATP hydrolysis. *J. Biol. Chem.* **276,** 47411–47420
39. Manolson, M. F., Proteau, D., and Jones, E. W. (1992) Evidence for a conserved 95–120-kDa subunit associated with and essential for activity of V-ATPases. *J. Exp. Biol.* **172,** 105–112
40. Rothman, J. H., and Stevens, T. H. (1986) Protein sorting in yeast: mutants defective in vacuole biogenesis mislocalize vacuolar proteins into the late secretory pathway. *Cell* **47,** 1041–1051
41. Kirisako, T., Baba, M., Ishihara, N., Miyazawa, K., Ohsumi, M., Yoshimori, T., Noda, T., and Ohsumi, Y. (1999) Formation process of autophagosome is traced with Apg8/Aut7p in yeast. *J. Cell Biol.* **147,** 435–446
42. Brauer, M. J., Yuan, J., Bennett, B. D., Lu, W., Kimball, E., Botstein, D., and Rabinowitz, J. D. (2006) Conservation of the metabolomic response to starvation across two divergent microbes. *Proc. Natl. Acad. Sci. U.S.A.* **103,** 19302–19307
43. Sancak, Y., Peterson, T. R., Shaul, Y. D., Lindquist, R. A., Thoreen, C. C., Bar-Peled, L., and Sabatini, D. M. (2008) The Rag GTPases bind raptor and mediate amino acid signaling to mTORC1. *Science* **320,** 1496–1501
44. Zoncu, R., Bar-Peled, L., Efeyan, A., Wang, S., Sancak, Y., and Sabatini, D. M. (2011) mTORC1 senses lysosomal amino acids through an inside-out mechanism that requires the vacuolar H^+-ATPase. *Science* **334,** 678–683
45. Bonfils, G., Jaquenoud, M., Bontron, S., Ostrowicz, C., Ungermann, C., and De Virgilio, C. (2012) Leucyl-tRNA synthetase controls TORC1 via the EGO complex. *Mol. Cell* **46,** 105–110
46. Faulhammer, F., Kanjilal-Kolar, S., Knödler, A., Lo, J., Lee, Y., Konrad, G., and Mayinger, P. (2007) Growth control of Golgi phosphoinositides by reciprocal localization of sac1 lipid phosphatase and pik1 4-kinase. *Traffic* **8,** 1554–1567
47. Hendricks, K. B., Wang, B. Q., Schnieders, E. A., and Thorner, J. (1999) Yeast homologue of neuronal frequenin is a regulator of phosphatidylinositol-4-OH kinase. *Nat. Cell Biol.* **1,** 234–241
48. Demmel, L., Gravert, M., Ercan, E., Habermann, B., Müller-Reichert, T., Kukhtina, V., Haucke, V., Baust, T., Sohrmann, M., Kalaidzidis, Y., Klose, C., Beck, M., Peter, M., and Walch-Solimena, C. (2008) The clathrin adaptor Gga2p is a phosphatidylinositol 4-phosphate effector at the Golgi exit. *Mol. Biol. Cell* **19,** 1991–2002
49. Daboussi, L., Costaguta, G., and Payne, G. S. (2012) Phosphoinositide-mediated clathrin adaptor progression at the trans-Golgi network. *Nat. Cell Biol.* **14,** 239–248
50. Puertollano, R., Randazzo, P. A., Presley, J. F., Hartnell, L. M., and Bonifacino, J. S. (2001) The GGAs promote ARF-dependent recruitment of clathrin to the TGN. *Cell* **105,** 93–102
51. Zhdankina, O., Strand, N. L., Redmond, J. M., and Boman, A. L. (2001) Yeast GGA proteins interact with GTP-bound Arf and facilitate transport through the Golgi. *Yeast* **18,** 1–18
52. Zhu, Y., Traub, L. M., and Kornfeld, S. (1998) ADP-ribosylation factor 1 transiently activates high-affinity adaptor protein complex AP-1 binding sites on Golgi membranes. *Mol. Biol. Cell* **9,** 1323–1337
53. Crottet, P., Meyer, D. M., Rohrer, J., and Spiess, M. (2002) ARF1-GTP, tyrosine-based signals, and phosphatidylinositol 4,5-bisphosphate constitute a minimal machinery to recruit the AP-1 clathrin adaptor to membranes. *Mol. Biol. Cell* **13,** 3672–3682
54. Perzov, N., Padler-Karavani, V., Nelson, H., and Nelson, N. (2002) Characterization of yeast V-ATPase mutants lacking Vph1p or Stv1p and the effect on endocytosis. *J. Exp. Biol.* **205,** 1209–1219
55. Furuta, N., Fujimura-Kamada, K., Saito, K., Yamamoto, T., and Tanaka, K. (2007) Endocytic recycling in yeast is regulated by putative phospholipid translocases and the Ypt31p/32p-Rcy1p pathway. *Mol. Biol. Cell* **18,** 295–312
56. Liu, K., Surendhran, K., Nothwehr, S. F., and Graham, T. R. (2008) P4-ATPase requirement for AP-1/clathrin function in protein transport from the trans-Golgi network and early endosomes. *Mol. Biol. Cell* **19,** 3526–3535
57. Dechant, R., Binda, M., Lee, S. S., Pelet, S., Winderickx, J., and Peter, M. (2010) Cytosolic pH is a second messenger for glucose and regulates the PKA pathway through V-ATPase. *EMBO J.* **29,** 2515–2526
58. Podbilewicz, B., and Mellman, I. (1990) ATP and cytosol requirements for transferrin recycling in intact and disrupted MDCK cells. *EMBO J.* **9,** 3477–3487
59. Liao, J. F., and Perkins, J. P. (1993) Differential effects of antimycin A on endocytosis and exocytosis of transferrin also are observed for internalization and externalization of β-adrenergic receptors. *Mol. Pharmacol.* **44,** 364–370
60. Clarke, B. L., and Weigel, P. H. (1985) Recycling of the asialoglycoprotein receptor in isolated rat hepatocytes: ATP depletion blocks receptor recycling but not a single round of endocytosis. *J. Biol. Chem.* **260,** 128–133
61. Suzuki, K. (2013) Selective autophagy in budding yeast. *Cell Death Differentiation* **20,** 43–48
62. Li, M., Khambu, B., Zhang, H., Kang, J. H., Chen, X., Chen, D., Vollmer, L., Liu, P. Q., Vogt, A., and Yin, X. M. (2013) Suppression of lysosome function induces autophagy via a feedback down-regulation of MTOR complex 1 (MTORC1) activity. *J. Biol. Chem.* **288,** 35769–35780
63. Barth, S., Glick, D., and Macleod, K. F. (2010) Autophagy: assays and artifacts. *J. Pathol.* **221,** 117–124
64. Juhász, G. (2012) Interpretation of bafilomycin, pH neutralizing or protease inhibitor treatments in autophagic flux experiments: novel considerations. *Autophagy* **8,** 1875–1876
65. Klionsky, D. J., Abdalla, F. C., Abeliovich, H., Abraham, R. T., Acevedo-Arozena, A., Adeli, K., Agholme, L., Agnello, M., Agostinis, P., Aguirre-Ghiso, J. A., and Ahn, H. J. (2012) Guidelines for the use and interpretation of assays for monitoring autophagy. *Autophagy* **8,** 445–544
66. Indge, K. J. (1968) Polyphosphates of the yeast cell vacuole. *J. Gen. Microbiol.* **51,** 447–455
67. Wilson, W. A., Wang, Z., and Roach, P. J. (2002) Systematic identification of the genes affecting glycogen storage in the yeast *Saccharomyces cerevisiae*: implication of the vacuole as a determinant of glycogen level. *Mol. Cell. Proteomics* **1,** 232–242